JOURNAL OF AGRICULTURAL AND FOOD CHEMISTRY

Water and Moisture Susceptibility of Chitosan and Paper-Based Materials: Structure–Property Relationships

N. BORDENAVE, S. GRELIER, F. PICHAVANT, AND V. COMA*

UMR US2B, Unité des Sciences du Bois et des Biopolymères, Université Bordeaux 1, INRA, CNRS, 351, cours de la Libération F-33405 Talence, France

Environmentally friendly and potentially bioactive food packaging based on chitosan-coated papers were elaborated. The morphology and the microstructure of these new materials were characterized by infrared spectroscopy and scanning electron microscopy. These observations suggested that the chitosan penetrated deeply into the paper, embedding the cellulose fibers, instead of forming a layer as expected. Through the barrier properties against moisture, the liquid water sensitivity, and NMR-relaxometry measurements, the water interactions were evaluated on the chitosan films and the chitosan-coated papers. They revealed that the coating by a chitosan film forming solution improved the paper moisture barrier properties but the surface hydrophilicity remained high. Relaxometry studies showed that, due to its hydrophilic character, chitosan controlled the interaction with water, despite the very low amount of deposit. On the other hand, the mechanical properties of papers were unmodified by the chitosan coating, which did not fundamentally affect the solid structure of the papers.

KEYWORDS: Paper; chitosan coating; biopolymer; food packaging; relaxometry; T_2; $T_{1\rho}$

INTRODUCTION

Food-borne disease has always topped the list of food safety concerns for most health agencies around the world. Contaminations of foods by pathogenic microorganisms are a major public health issue, and among other solutions, the use of bioactive packaging systems is a potentially efficient answer to this problem.

In parallel, environmental concerns including the limitation of CO_2 emissions, and the presumably increasing cost of petrochemicals, have made renewable resources more interesting as substitutes for synthetic packaging materials for food preservation applications.

In this respect, the use of paper and cardboard might be increased if their moisture-barrier properties could be improved. Today, these properties are often obtained by the association of a paper matrix with a synthetic polymer. Unfortunately this association leads to a loss of two fundamental interests of the paper-based packaging: easy recyclability and sustainability or biodegradability. Therefore, this study aims to elaborate bioactive paper-based packaging materials, while maintaining their recycling and biodegradation aptitude. In this respect, the association of papers and film forming solutions derived from natural antimicrobial macromolecules was studied. Chitosan was selected, because of its good film forming properties and its antimicrobial activity, in particular against pathogenic strains potentially found in the foodstuffs (*1–3*). Chitosan is a linear aminopolysaccharide derived from chitin, a major component of insects and crustacean shells. Obviously, it is biodegradable and environmentally friendly (*4, 5*). The presence of amino groups makes chitosan soluble in dilute aqueous solutions of common weak acids. The cationic character of the dissolved chitosan is known to provide a biological activity against several food strains (*6, 7*). Some studies have reported the use of chitosan coatings for fruits and other food products. They discussed mechanical, antimicrobial and organoleptic properties, oxygen and moisture permeability, gloss, and wettability (*8–10*). The moisture-barrier properties of biopolymer-based materials for food packaging have been also widely studied (*11–13*) and demonstrated their efficiency against food deterioration.

This study focuses on the comparative properties of chitosan films and chitosan-coated papers or cardboards. The characterization of the materials was first achieved by scanning electron microscopy and infrared spectroscopy (*14, 15*). Second, the impact of the chitosan coating on the moisture and water sensitivity of these materials was particularly studied. Fundamental characterization of the materials by means of the behavior of water in this latter study was then conducted by T_2 NMR-relaxometry. Indeed, the characterization of water behavior in chitosan films (*16–19*), papers, or chitosan-coated papers (*20, 21*) could help to understand their barrier properties. Third, mechanical properties were also determined, as far as they are important characteristics of food packaging materials (*22–25*). This was correlated with the study of the solid matrix of the materials by $T_{1\rho}$ NMR-relaxometry.

* Author to whom any correspondence should be addressed. Fax: 33 5 56 84 64 22. E-mail: v.coma@us2b.u-bordeaux1.fr.

10.1021/jf070595i CCC: $37.00
Published on Web 10/23/2007

MATERIALS AND METHODS

Materials. Chitosan 244 (deacetylation degree higher than 95%, Mw = 400 kDa) was provided by France Chitine (Marseille, France). Acetic acid (purity ≥ 99.5%) was provided by Sigma-Aldrich (St Quentin Fallavier, France). In the project framework, papers were provided by Ahlstrom (Ascoflex 40, noncalendered, one side minerally pretreated, 40 $g \cdot m^{-2}$, 48 μm thick, Grenoble, France) and Stora Enso (Performa Nature 320, noncalendered, one side minerally pretreated, 320 $g \cdot m^{-2}$, 344 μm thick, Helsinki, Finland).

Methods. *Elaboration of Chitosan Films.* Here, 2% (w/w) chitosan film forming solutions were obtained by dispersing the chitosan in a 1% aqueous acetic acid solution. After mixing, the solution was degassed under vacuum and cast in a polyethylene Petri dish and then dried at room temperature and relative humidity (RH) for 12 h. The films were conditioned in a controlled atmosphere (23 ± 1 °C and 50 ± 5% RH) for at least 5 days before the property measurements were taken.

Elaboration of Chitosan-Coated Papers. Stora Enso and Ahlstrom papers were coated with the chitosan film forming solution mentioned above (2% w/w in a 1% aqueous solution of acetic acid), using a coating table (K101 Control Coater, Erichsen, Rueil-Malmaison, France) at room temperature and equipped with a 120 μm blade. A 5 mL portion of the solution corresponding to a deposit of 0.1 g of dry chitosan on a 2.5 g sheet of Ahlstrom paper or a 20 g sheet of Stora Enso paper (210 × 297 mm format sheet) was layered on the untreated side by mineral coating, corresponding to a deposit of about 1.6 $g \cdot m^{-2}$: 40 mg of chitosan/g of Ahlstrom paper and 5 mg of chitosan/g of Stora Enso paper. The coated materials were subsequently conditioned at 23 ± 1 °C and 50 ± 5% RH for 5 days before achieving property measurements.

Scanning Electron Microscopy (SEM) Observations. Film and paper samples were cut and placed onto specimen supports to obtain surface and transversal views. After the gold and palladium coating procedure, samples were viewed using a Jeol 840A microscope (Jeol Europe, Croissy-sur-Seine, France).

Fourier Transform Infrared (FTIR) Spectroscopy Analysis. FTIR analyses were performed to study the coated papers. Reflection and attenuated total reflection (ATR) spectra were recorded by a ThermoNicolet AVATAR 370 FTIR coupled with a Nicolet Centaurus IR-microscope, with a Silicium ATR crystal, and treated by OMNIC software (Thermo-Nicolet, Courtaboeuf, France), between 400 and 4000 cm^{-1} using 50 scans at a resolution of 4 cm^{-1}.

Thickness Measurements. Material thickness was determined with a micrometer Lorentzen & Wettre SE050 (Lorentzen & Wettre, Saint-Germain-en-Laye, France), from six measurements per material.

Water Vapor Transfer Rate (WVTR) Determination. The WVTR of chitosan-based materials was evaluated using method NF ISO 2528 (1995). Briefly, an aluminum cup containing anhydrous $CaCl_2$ desiccant was sealed by the test material (50 cm^2 exchange area) with paraffin wax at 50 °C. It was placed in an environment of controlled RH and temperature (50 ± 5% RH and 23 ± 1 °C). The mineral side of the paper faced outwards at all times.

The WVTR ($g \cdot m^{-2} \cdot d^{-1}$) was determined from the weight increase of the cup over time at the steady state of transfer using the following equation:

$$\mathrm{WVTR} = \frac{\Delta m \times 24}{\Delta t \times S}$$

where Δm is the amount of H_2O vapor passing through a material area S during time Δt determined by weight change of the cups vs time. Plotted-linear regression was used to calculate the slope of a fitted straight line.

Control cups, without the anhydrous $CaCl_2$ desiccant were conducted in parallel. Their weight gain or loss is used as a correcting factor of the tested cups.

The WVTR was given at atmospheric pressure (1 atm) with a RH gradient of 0–50%.

Relaxometry NMR Analysis. NMR measurements were carried out on a Bruker Minispec PC120 spectrometer (Bruker Optics, Champ-sur-Marne, France) operating at 20 MHz proton resonance frequency corresponding to a magnetic field of 0.47 T. The $\pi/2$ pulse length is 2.8 μs, and the typical value of dead time is 7 μs. The temperature of the magnet was 40 °C and the probe temperature was initially regulated at 25 °C. Before each measurement, a duration of 30 min was allowed for temperature equilibration of the samples. Two different sequences of measurements were used: the Carr, Purcell, Meiboom, and Gill sequence (CPMG) for the T_2 study and the "spin–lock" sequence for the $T_{1\rho}$ study.

The CPMG sequence permits the characterization of the protons of the material by spin–spin relaxation times T_2. Spectra were acquired setting 600 echoes, with an accumulation of 1000 scans spaced out by a recycle delay of 3 s. Echo spacing of 30 ms is needed to discriminate the longest T_2 values attributed to the liquid part of the material. Usually, with the CPMG sequence, the echo amplitude detected at the time is given by the following: $M(t) = \sum_i k_i \exp^{-t/T_{2i}}$ where T_{2i} and k_i are respectively the spin–spin relaxation time and the weight of the ith component of the decay. Errors in reported T_{2i} are within 2% in nominal values. Multiexponential profiles obtained by this sequence are also fitted to a sum of exponential components and had to be decomposed into their different contributions. In this study, a continuous approach has been used for the decomposition of the magnetization decay, with CONTIN, a Provenchers' program.

The result of the calculation is a relaxation spectrum giving intensity versus relaxation time.

$T_{1\rho}$ measurements were performed with the spin–lock sequence and the same analytical process.

To study the moisture susceptibility of materials, the NMR study was conducted on samples previously conditioned in air-tight containers containing salt-saturated solutions at 25 °C to reach constant RH: LiCl–H_2O (12% RH), CH_3COOK–$1.5H_2O$ (22% RH), $MgCl_2$ (33% RH), K_2CO_3 (43% RH), $Mg(NO_3)_2$–$6H_2O$ (53% RH), $NaNO_3$ (65% RH), NaCl (75% RH), and KCl (85% RH).

Water Contact Angle Meter Determination. The contact angle between the material and a distilled water droplet was measured according to TAPPI T458 cm-94 (1994) and using a goniometer Krüss DSA 10Mk2 (Krüss, Palaiseau, France) equipped with a camera and a recording system. The resulting angle was calculated from 10 measurements.

Penetration Dynamic Analysis (PDA). A material sample is brought into contact with water in a measuring cell. From the moment of water contact, it is radiated in the Z-direction with high-frequency low-energy ultrasonic signals. These signals were received by a sensitive sensor, before they are processed in the device and treated by a computer. PDA was performed with an EMTEC PDA C02 apparatus (Emtec Electronic, Leipzig, Germany). The PDA curves (time vs percentage of transmission of the ultrasonic signals), showing the penetration speed of water through the materials, are the average curves calculated from three experiments. Transmission is 100% at $t = 0$ s.

Mechanical Property Measurements. Mechanical tests were performed on a MTS Systems Dy22b (MTS, Eden Prairie, MN) traction machine according to modified ISO 1924-2 (1995) at 23 ± 1 °C and 50 ± 5% RH. All the samples were cut to 2.5 cm × 6 cm and the elongation speed was 3 $mm \cdot min^{-1}$.Young's modulus, strain at break, and elongation at break were calculated. For the sheeted materials, all the tests were conducted in a longitudinal direction. Six replicates were analyzed for each material.

Statistical Treatment. All experiments were repeated at least three times. Data are mean values given with a Student's confidence interval at 95% probability ($p < 0.05$).

RESULTS AND DISCUSSION

Coating Analysis. *Scanning Electron Microscopy Study.* The SEM views are presented in **Figure 1**. Micrographs of Ahlstrom papers (**Figures 1a–c**) showed that chitosan penetrated into the paper, completely coated the cellulose fibers, and filled the pores of the paper. It can be assumed that Ahlstrom paper surface was saturated with chitosan. The penetration of the chitosan was confirmed on the cross-sectional views.

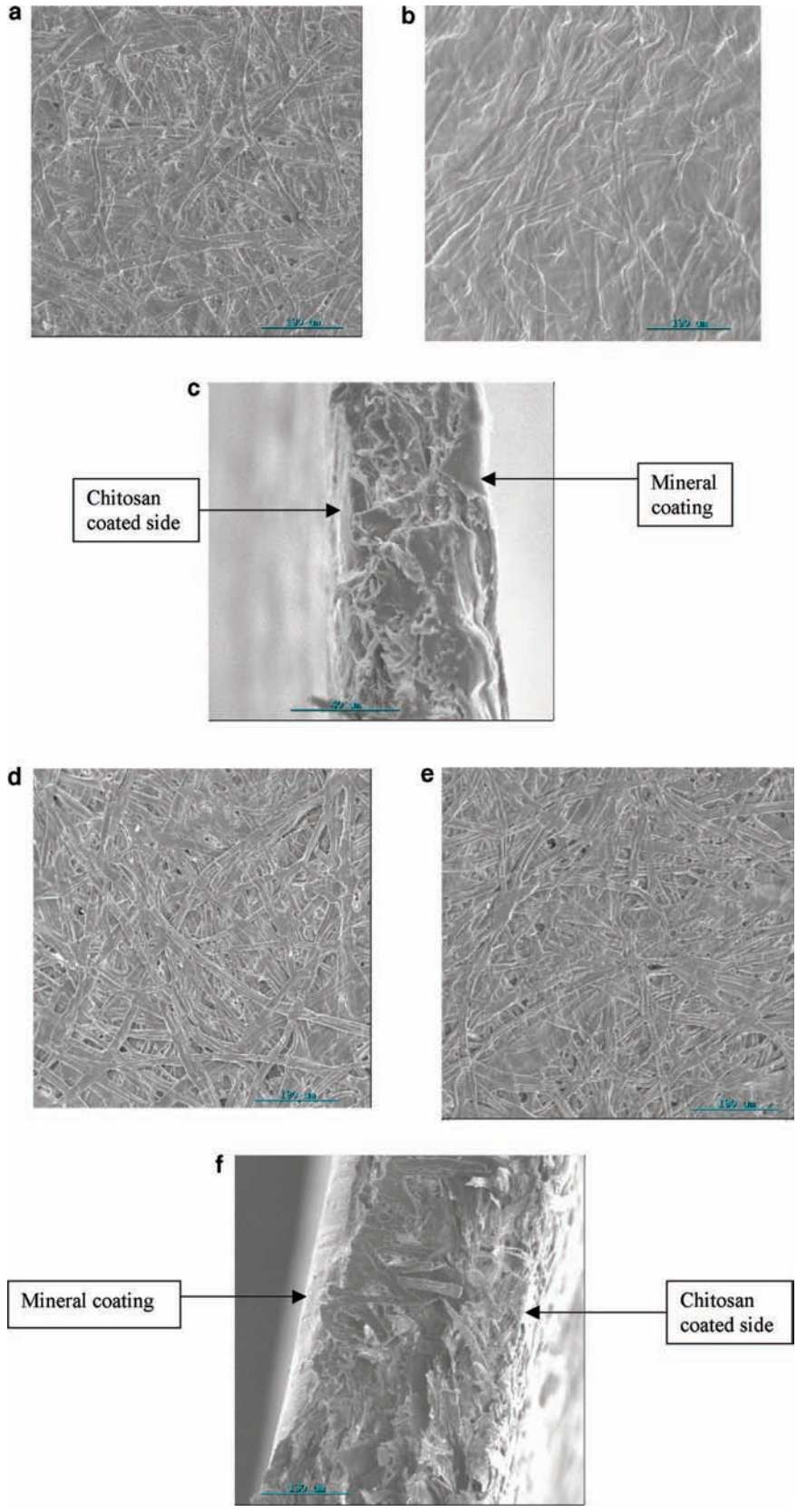

Figure 1. Microscopic views of the noncoated and chitosan-coated paper. (**a**) Microscopic surface view (×100) of the noncoated Ahlstrom paper observed from the coated side. (**b**) Microscopic surface view (×100) of the coated Ahlstrom paper from the coated side. (**c**) Microscopic side view (×600) of the section of Ahlstrom coated paper. (**d**) Microscopic surface view (×100) of noncoated StoraEnso paper observed from the nonpretreated side. (**e**) Microscopic surface view (×100) of StoraEnso coated paper from the coated side. (**f**) Microscopic side view (×150) of the section of StoraEnso coated paper.

Microscopic views of Stora Enso paper (**Figure 1d–f**) showed that surface pores were not completely filled with chitosan, allowing the conclusion that the paper surface was not saturated with chitosan.

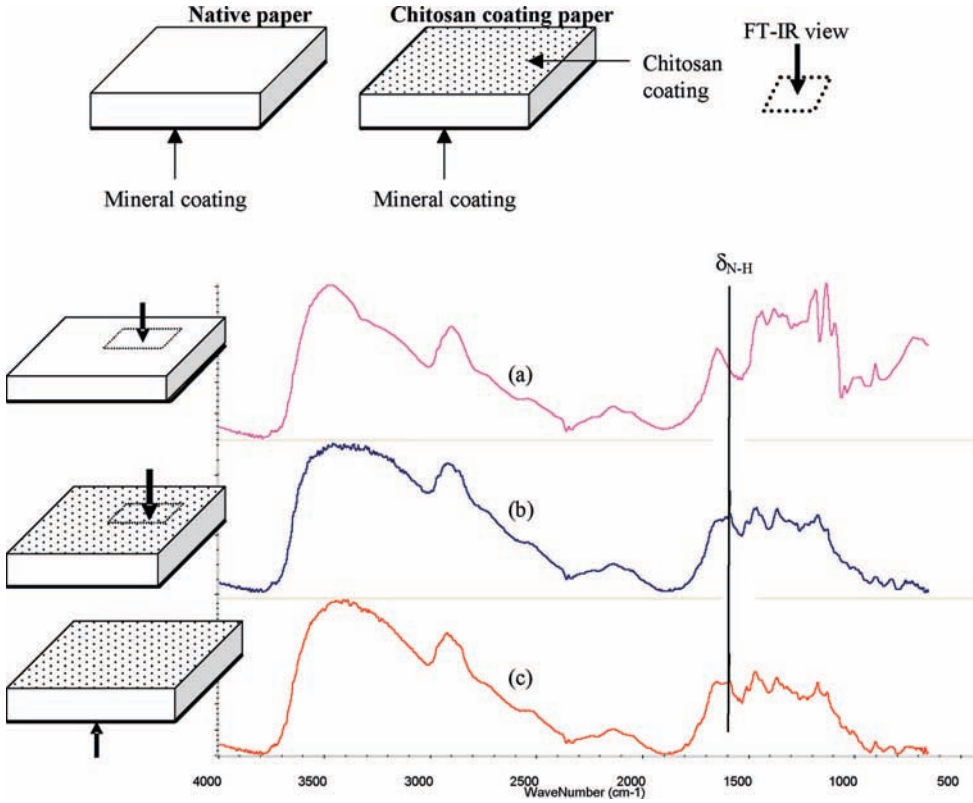

Figure 2. Pictograms for papers, coated papers and FTIR views, and FTIR-reflection spectra of Ahlstrom paper: (**a**) noncoated paper, paper side; (**b**) coated paper, coated side; (**c**) coated paper, opposite side of the coating.

To confirm these different observations, reflection-FTIR analyses were performed on both sides of uncoated and chitosan coated papers.

Fourier Transformed Infrared Spectroscopy Analyses. FTIR analyses were therefore carried out to detect the penetration of chitosan inside both selected papers, by using an aminopolysaccharide characteristic band of δ_{N-H} at 1576 cm^{-1}.

Figure 2 shows FTIR reflection spectra for Ahlstrom paper viewed from the paper side (**a**) and Ahlstrom paper coated with chitosan observed from the coated side (**b**) and from the mineral side (**c**). The 1576 cm^{-1} band was observed only on spectra **b** and **c**, revealing the presence of chitosan on both sides of the coated papers. This could be due to a penetration of the chitosan coating solution through the paper, leading to a presence of chitosan in the whole paper.

Figure 3 shows FTIR-ATR spectra for coated Ahlstrom paper viewed from the coated side (**a**) and from the mineral side (**b**) and uncoated Ahlstrom paper viewed from the mineral side (**c**). As spectrum **c** did not show a typical chitosan pattern such as observed in spectrum **a**, the chitosan did not completely cross the paper matrix. Indeed, the difference between reflection and ATR modes is the penetration depth of the IR beam in the material: in reflection mode, the IR beam penetrates through 15–20 μm, while in ATR mode the IR beam penetrates the material through about 5 μm. Thus, from the opposite side of the coating, chitosan was observed at a 15–20 μm depth in the paper (**Figure 2**) but was not observed any more at a 5 μm depth (**Figure 3**), and this corresponded approximately to the mineral layer thickness (**Figure 1c**). In conclusion, the chitosan penetrated deeply into the Ahlstrom paper down to the mineral layer, filling the pores and coating the cellulose fibers.

Figure 4 shows FTIR-reflection spectra for Stora Enso paper coated with chitosan observed from the coated side (**a**) and from the mineral side (**b**) and for the uncoated Stora Enso paper viewed from the mineral side (**c**) and the paper side (**d**). On coated papers, chitosan was not observed from the opposite side of the coating, unlike on the Ahlstrom paper. Indeed, the mineral coating thickness is about of 40 μm in this paper. As in the Ahlstrom paper, this observation means that the chitosan solution soaked the paper but did not penetrate the mineral layer.

Figure 5 shows FTIR-reflection spectra of coated Stora Enso paper viewed from the coated side (**a**) and from the cross section (**b**). The latter was obtained from a 100-μm-large window of the microscope fixed at the middle of the observed cross section. Both spectra exhibited the characteristic peak of chitosan. That means that, for Stora Enso paper, as well as for Ahlstrom paper, chitosan penetrated into the mass of the paper, but micrographs in **Figure 1a** and **b** showed that this paper was not saturated with chitosan. Moreover, the relatively high paper thickness led to a lower ratio of chitosan/cellulose fibers into the material, compared to coated Ahlstrom paper.

The thicknesses of these materials are given in **Table 1**. Coated Ahlstrom paper was 8 μm thicker than the native paper, and coated Stora Enso paper was 58 μm thicker than the native paper. Such a difference in the thickness gains could be surprising, but it has been observed that the mineral layer of both papers was not affected by chitosan coating. Thus, we shall not consider it in the calculation of a thickness gain. Finally, without considering the mineral layer, Ahlstrom paper, coated Ahlstrom paper, Stora Enso paper, and coated Stora Enso paper were respectively 43, 51, 304, and 362 μm thick.

In this respect, Ahlstrom and Stora Enso papers thicknesses are both increased by 19%. This phenomenon could be due to the penetration of the aqueous chitosan solution in the cellulose fibers matrix. Indeed, the cellulose fibers are strained and maintained together in paper mainly by hydrogen bonds. The incorporation of water from the film forming solution would have lowered these interactions and would have allowed the swelling of the paper by relaxation of the strains and the introduction of chitosan between fibers. Thus, after drying and

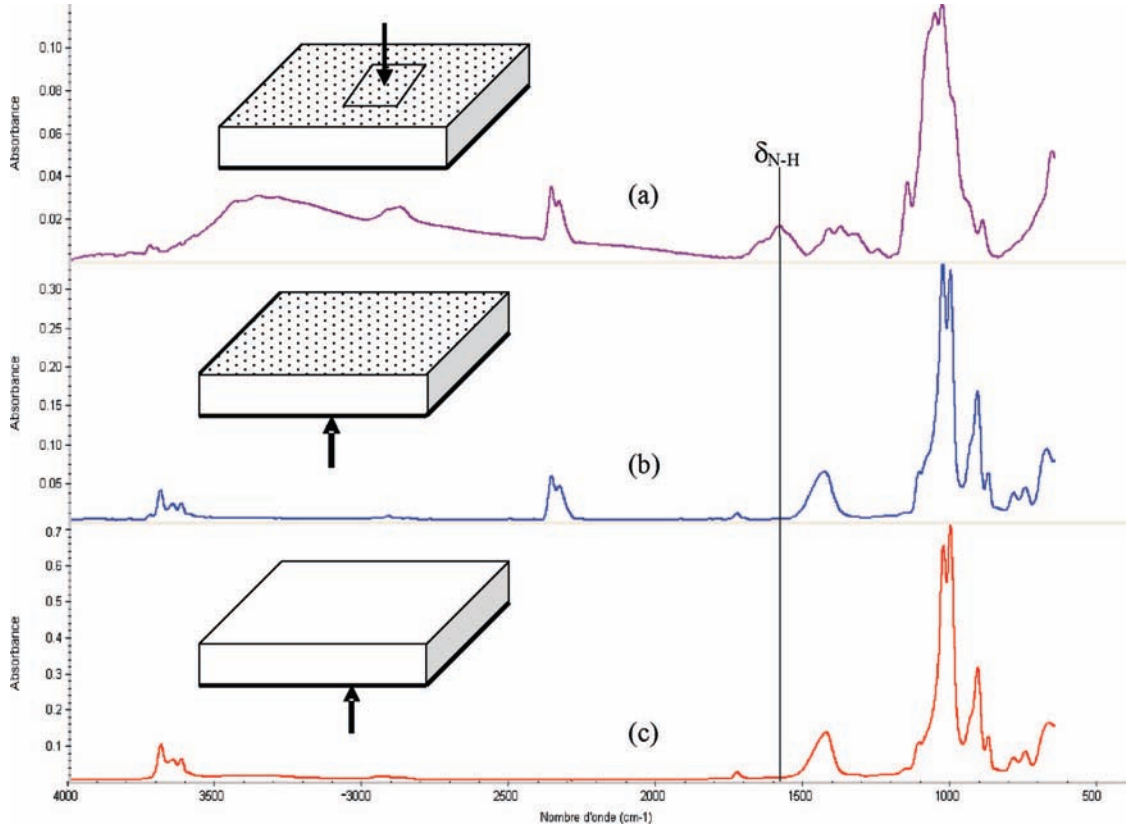

Figure 3. FTIR-ATR spectra of the Ahlstrom paper: (**a**) chitosan-coated paper observed from the coated side, (**b**) chitosan-coated paper observed from the mineral side, (**c**) paper observed from the mineral side.

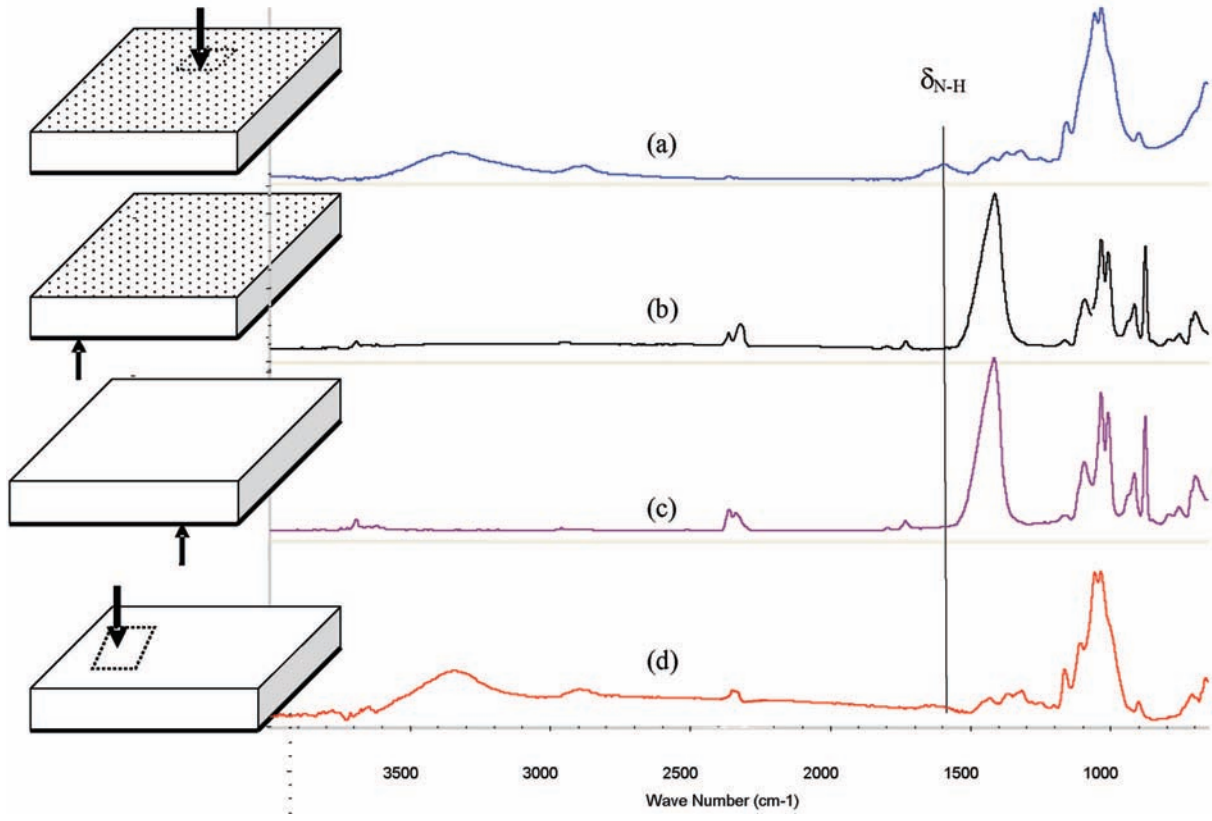

Figure 4. FTIR-ATR spectra of Stora Enso: (**a**) coated paper, observed from the coated side; (**b**) coated paper, observed from the mineral side; (**c**) uncoated paper observed from the mineral side; (**d**) uncoated paper, observed from the paper side.

without calendering, the previous interfiber interactions could have been perturbed by chitosan and the fibers would not be strained anymore. It would have led to an increase of the papers thickness proportional to their original thickness: the main driving force of this phenomenon would be the breaking of strains by water, and even for low chitosan/cellulose ratios as

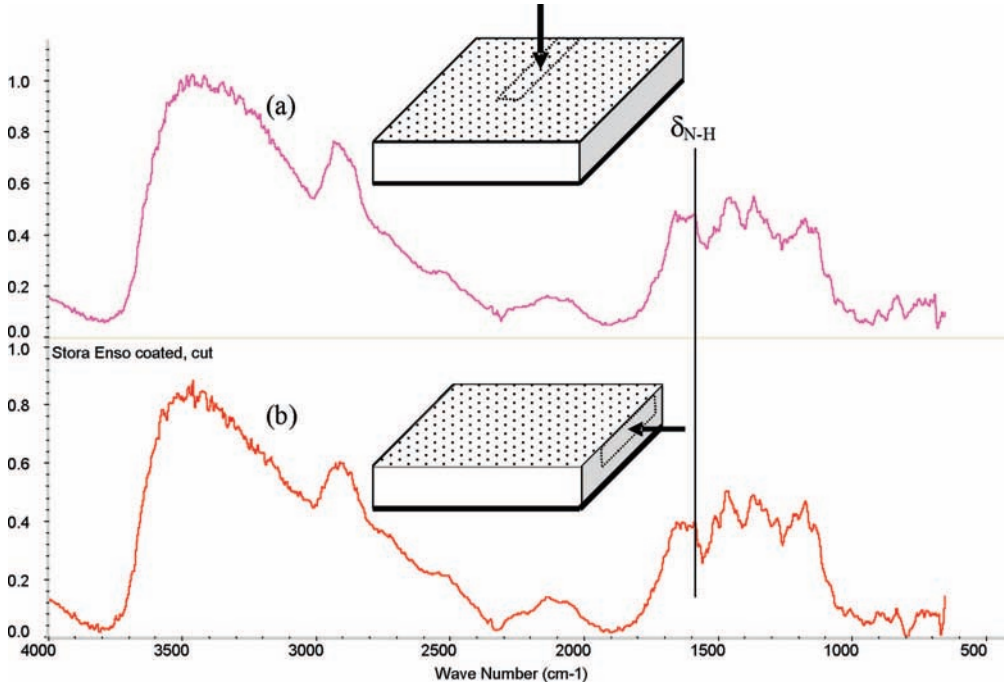

Figure 5. FTIR-reflection spectra of coated Stora Enso paper: (**a**) viewed from coated side and (**b**) viewed from the cross section.

Table 1. Moisture-Barrier Properties of the Different Materials for Modeling Dry Food and Wet Food[a]

	thickness (μm)	WVTR 50% RH ($g \cdot m^{-2} \cdot d^{-1}$)
chitosan film	21 ± 3	63 ± 12
Ahlstrom paper	48 ± 1	643 ± 33
coated Ahlstrom paper	56 ± 1	241 ± 16
StoraEnso paper	344 ± 1	344 ± 35
coated StoraEnso paper	402 ± 2	161 ± 41

[a] The means of thickness and WVTR were calculated from six and three repetitions, respectively. Standard deviations were calculated with a Student's *t*-test ($p < 0.05$).

in the Stora Enso paper, it would be sufficient to prevent the cellulose from regaining its initial state. Indeed, chitosan is a positively charged polymer, while cellulose is potentially negatively charged in papers: only a small amount of chitosan can lead to electrostatic perturbations.

In conclusion, if papers are considered as networks of cellulose fibers with pores, the coated papers can be assimilated into networks of cellulose fibers embedded with chitosan, with pores more or less filled with chitosan.

Consequently, the macroscopic properties of these materials (as packaging materials) shall be affected by these changes in their structure. A major property that has to be tested for applications in food packaging materials is its resistance to moisture transfer.

Water Vapor Barrier. Experiments were conducted at $50 \pm 5\%$ RH and $85 \pm 5\%$ RH, but some materials did not withstand high moisture levels without degradation (chitosan films and chitosan-coated Ahlstrom paper). Therefore, only the results for $50 \pm 5\%$ RH and 23 ± 1 °C were presented.

The WVTR of chitosan films and coated papers, proposed in **Table 1**, showed that the chitosan coating led to a significant decrease of the paper moisture transfer. The transfer reduction for the Ahlstrom paper was of about 62.5%. The WVTR for the Stora Enso paper was reduced by about 53.2%.

This could be explained by the microstructure of the coated papers. As observed previously, the paper thickness increased after the coating and many of their pores are filled by chitosan. Thus, the preferential ways for water to cross the materials were lengthened and obstructed, and this could explain the decrease of moisture tranfer.

A better understanding of the interaction of water and these materials by T_2 NMR-relaxometry would help to more precisely interpret this phenomenon.

***T_2* Measurements by Low Resolution NMR.** The T_2 parameter probes the fast motion interactions between motionally "free" water molecules (liquid phase) and their local macromolecular environment by spin–spin relaxation. Thus, this parameter could be used to identify their different states of water in a material (bound or free water).

Typically, two domains were observed on relaxation-NMR spectra: The first, with a peak in the lowest relaxation times, is an echo of the solid phase, attributed to the hydrogen atoms of the matrix. The latter gives no discerning information and can disappear sometimes. The second part of the relaxometry NMR spectrum showed peaks at higher relaxation times according to the mobility of water (bound to free) in a material. Only this part was studied, depending on the RH where they were conditioned (related to the water content of the samples).

NMR spectra for the Ahlstrom paper, presented in the **Figure 6**, contained two different zones of RH. The first zone, between 12 and 65% RH, exhibited one peak between 0.05 and 0.2 ms attributed to the first water layers tightly bound to the cellulose fibers of the paper. The second zone, between 75 and 85% RH, showed a new peak around 2 ms of less bound water which could be attributed to the water filling the pores of the paper.

NMR spectra of the chitosan films presented in **Figure 7** show radically different behavior. As for the paper matrix, two zones of RH were observed. The first zone for 12–53% RH showed only the solid echo: no mobile water can be observed at these RHs. In the second zone, between 65 and 85% RH, one peak of water with low mobility appeared, probably bound to chitosan. Indeed, water would be tightly bound at the surface of the hydrophilic polymer chains at low RH, with solid phase behavior: the relaxation times of water protons and chitosan protons would be similar. For higher RH values, the water excess would be more mobile but still trapped in the chitosan

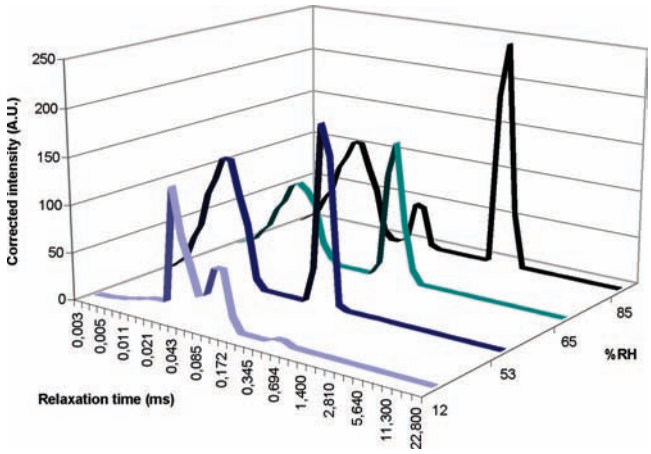

Figure 6. T_2 relaxation spectra of Ahlstrom paper at 12, 53, 65, and 85% RH from foreground to background.

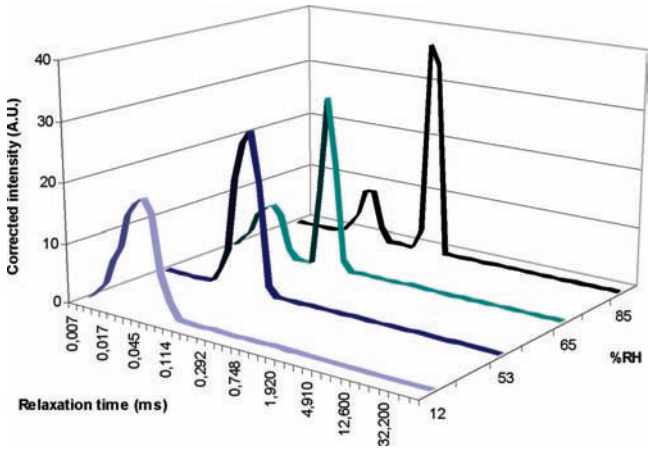

Figure 7. T_2 relaxation spectra of chitosan films at 12, 43, 65, and 85% RH from foreground to background.

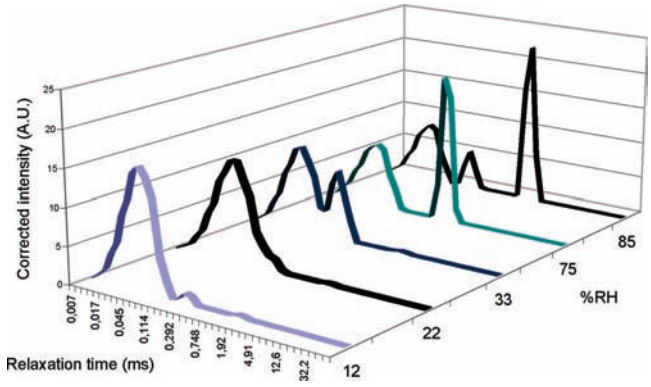

Figure 8. T_2 relaxation spectra of chitosan films at 12, 22, 33, 75, and 85% RH from foreground to background.

network, therefore exhibiting higher relaxation times and transforming the system into an hydrogel.

The chitosan-coated Ahlstrom paper spectrum is presented in **Figure 8**. A significant difference was observed between the behavior of the paper and the coated papers. According the storage RH, three zones were observed. The first one, 12–22% RH, showed only the solid echo. The second one, 33–75% RH, showed one peak: as observed in the material microstructure, the cellulose fibers were embedded with chitosan. Thus, water could not be directly bound to these latter, and this peak would be due to the chitosan hydrogel formation. The last zone, around 85% RH, led to a new peak of less bound water probably due to the filling of the paper pores. As a result, these transitions are slightly modified compared to the behavior of paper.

Thus, T_2 measurements showed that the chitosan coating changed and drove the behavior of the paper, through humidity, despite the very low quantity of chitosan coating (about 1.6 $g \cdot m^{-2}$ of paper).

This behavior could be correlated to the macroscopic property as described above. Indeed, as NMR-relaxometry showed in static phenomena, water is preferentially bound to chitosan rather than being mobile as in the pores of native paper. Thus, in dynamic phenomena, the chitosan coating decreased the WVTR of papers, due to the filling of the pores as a preferential way for water to cross the materials and due to the thickness increase of the materials.

Further investigations on these materials as food packaging materials were then conducted to study the interactions between biomaterials and liquid water.

Table 2. Initial Drop Angle and Penetration Speed of the Water on the Different Materials[a]

	thickness (μm)	initial drop angle (deg)
chitosan film	21 ± 3	101 ± 6
Ahlstrom paper	48 ± 1	129 ± 6
coated Ahlstrom paper	56 ± 1	78 ± 8
Stora Enso paper	344 ± 1	84 ± 3
coated Stora Enso paper	402 ± 2	83 ± 6

[a] Means were calculated from 10 repetitions. Standard deviations were calculated with a Student's *t*-test ($p < 0.05$).

Liquid Water Interactions. The previous observations showed that the chitosan coating slowed down the water vapor transmission despite its hydrophilic character. The consequences on the surface tension of the materials of the incorporation of such a hydrophilic component had to be studied. Thus, in this section, the papers were tested on the nonpretreated side, whether coated with chitosan or not. The results are presented in **Table 2**.

The native Ahlstrom paper exhibited a hydrophobic character (129°), due to the sizing process. The contact angle on Stora Enso paper conforms more to the hydrophilic character than can be expected from cellulose (84°). However, whatever the contact angles values before coating, it reached an average value of around 80° after the coating, for both papers. As previously observed, chitosan embedded cellulose fibers and partly filled the pores of the papers, reducing the effects of sizing and giving hydrophilic character to the surfaces of the coated papers.

The PDA analyses presented in **Figure 9** show that, for Ahlstrom paper, the wetting time, initially 13 s, completely disappeared after the chitosan coating. Moreover, as expected, the water penetration speed was highly increased. Indeed, paper can be considered as a network of cellulose fibers and pores. Thus, in the native paper, these pores act as gaps slowing down the penetration of liquid water through this discontinuous material. On the other hand, on SEM micrographs, the coated paper seemed to be saturated with chitosan, with its pores completely filled. Thus, liquid water could penetrate faster through this continuous and hydrophilic material.

It could also be observed that the chitosan coating decreased the wetting time of the Stora Enso paper from 3.5 to 1.7 s, without significant modification of the water penetration speed (given by the curves slopes). Indeed, due to the lower chitosan–paper ratio (about 5 mg of chitosan for 1 g of paper), only a few pores are filled with chitosan. Thus, liquid water would be conducted through discontinuous materials, with pores slowing down its penetration, as in native Stora Enso paper.

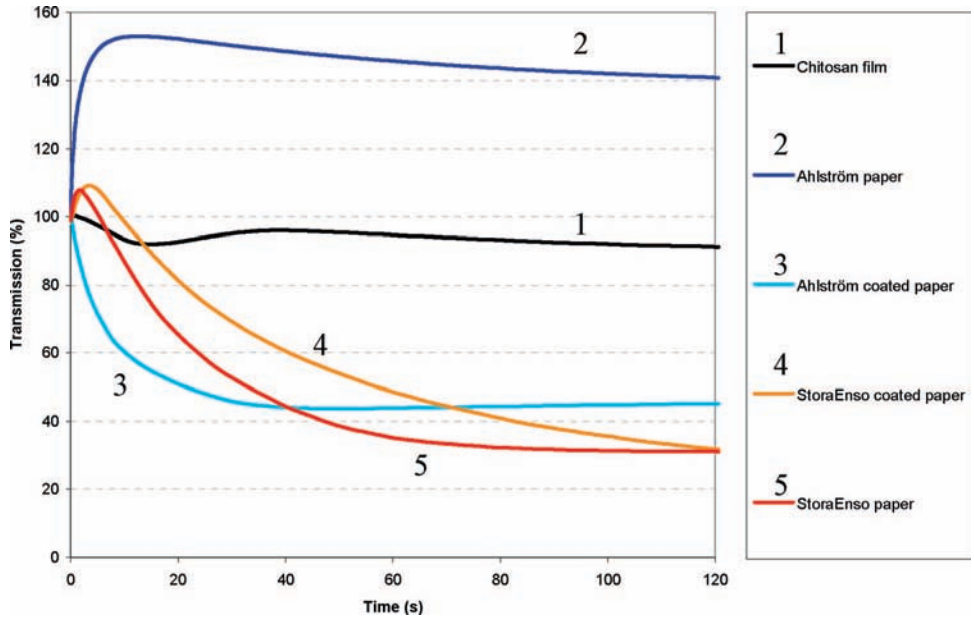

Figure 9. PDA curves showing the transmission (%) of ultrasonic signals vs time through the different materials.

Table 3. Mechanical Properties of Materials[a]

	thickness (μm)	tensile stress		
		Young's modulus (GPa)	ultimate elongation (%)	tensile strength (MPa)
chitosan film	19 ± 1	18.0 ± 2.0	7.0 ± 0.9	6 ± 1
Ahlstrom paper	48 ± 1	3.6 ± 0.3	3.0 ± 0.5	54 ± 1
Ahlstrom paper coated with chitosan	56 ± 1	1.7 ± 0.3	2.9 ± 0.1	48 ± 2
Stora Enso paper	344 ± 1	3.0 ± 0.1	2.8 ± 0.1	49 ± 1
Stora Enso paper coated with chitosan	402 ± 2	2.8 ± 0.9	3.0 ± 0.1	41 ± 1

[a] Means were calculated from 6 repetitions. Standard deviations were calculated with a Student's *t*-test ($p < 0.05$).

It is noticeable that the values of the wetting times for native Ahlstrom and Stora Enso papers confirm the measured contact angles: this wetting time is 3.7 times higher for Ahlstrom paper, revealing its surface hydrophobicity.

In conclusion, as expected, the incorporation of a highly hydrophilic component such as chitosan increased the surface tension of the materials and made them more sensitive to liquid water penetration.

Due to potential food applications of this biopackaging, other properties of the materials need to be tested, such as mechanical properties.

Mechanical Tests. The positive impact of a chitosan coating on the barrier properties of paper-based materials increases their potential for food applications. But, the microstructure observations showed changes in the cellulose fibers network, which is responsible for the mechanical properties of the papers. It was therefore necessary to check that the aqueous coating would not lead to a decrease in the mechanical properties of paper-based materials.

Table 3 shows that, for Ahlstrom paper, a slight decrease in the Young's modulus parameter appeared, leading to the appearance of a slight plastic phase. It has been assumed previously that the chitosan coating led to a permanent relaxation of the cellulose fibers strains. Moreover, the positively charged chitosan was introduced between the potentially negatively charged cellulose fibers, perturbing their interactions and their cohesion. Thus, it can be assumed that in Ahlstrom paper, chitosan potentially acted as a plasticizer, leading to a reduction of the Young's modulus.

On the other hand, the mechanical properties remained almost unchanged for Stora Enso paper. Indeed, this paper was impregnated by the chitosan solution and swelled, but the cohesion of its fibers network seems to be unaffected by this phenomenon, perhaps because of the very low amount of chitosan (5 mg/g of paper): the paper would have swelled because of the relaxation of the cellulose fibers due to water impregnation, but the chitosan introduced between them was not in sufficient amount to act as an efficient plasticizer and the mechanical properties of the materials would have remained unchanged.

In conclusion, except the slight decrease of the Young's modulus for Ahlstrom paper, no dramatic changes in the mechanical properties were obtained after a chitosan coating for both papers. Indeed, the paper could be considered as a system of cellulose fibers and pores, and mechanical properties are thus in relation with this solid matrix. This system is slightly modified by the introduction of chitosan, but the cellulose fibers network still seemed to drive the mechanical behavior of the materials. The study of the impact of the chitosan coating on the solid matrix could therefore be of some interest.

***$T_{1\rho}$* Measurements by Low Resolution NMR.** The $T_{1\rho}$ parameter probes the slow motion interactions between motionally restricted water molecules (solid phase) and their local macromolecular environment by spin–lattice relaxation. Thus, this parameter gives indirect information about the hydrogen atom mobility in the solid phases of the samples.

Once again, there were typically two domains that could be observed on the relaxation $T_{1\rho}$ NMR spectra: the first one, in the lowest relaxation times, is called "solid echo" and is attributed to the relaxation processes of various kinds of protons of the solid phase of the material with extremely short relaxation times. It could not be interpreted as physical data related to the material, and it can disappear sometimes. The second part showed peaks at higher relaxation times in relation to the hydrogen atoms of the solid matrix: only this part was studied depending on the water content of the samples. As a result, the

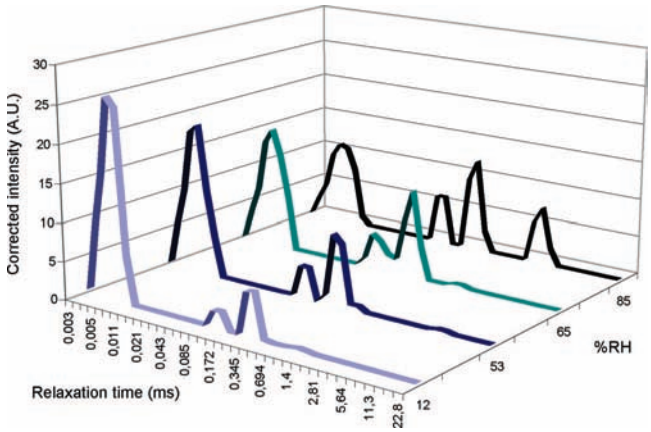

Figure 10. $T_{1\rho}$ relaxation spectra of Ahlstrom paper at 12, 22, 33, and 85% RH from foreground to background.

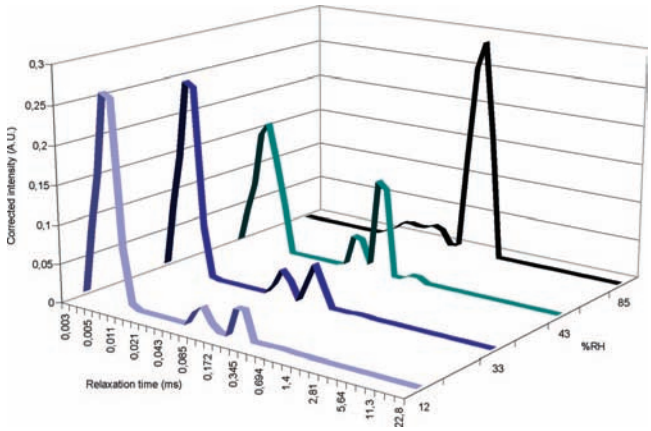

Figure 11. $T_{1\rho}$ relaxation spectra of chitosan films at 12, 33, 43, and 85% RH from foreground to background.

mobility of cellulose or chitosan chains in a material will be studied in the second part of the relaxometry $T_{1\rho}$ NMR spectrum.

NMR spectra for Ahlstrom paper are presented in **Figure 10**, exhibiting two peaks (peak no. 1 around 0.1 and peak no. 2 around 0.3 ms) which might be due to crystalline and amorphous cellulose in the paper, the amorphous chains being more mobile. Over the whole range of RH, this was almost constant. From 65 to 85% RH, a peak related to higher relaxation times appeared. This could be due to a higher mobility of some parts of the cellulose fibers due to their hydration.

NMR spectra for chitosan films are presented in **Figure 11**. Over the whole range of RH, there is only one spectra pattern. As for papers, the same group of two peaks could be observed and no additional peak appeared at high RH. However, with increasing RH, the ratio of the intensities (I_{peak2}/I_{peak1}) was increased. This could be due to the release of strains on chitosan chains due to hydration followed by the formation of a hydrogel.

The chitosan-coated Ahlstrom paper spectra are presented in **Figure 12**. No significant difference was observed between the behavior of the paper and the coated papers. The first two peaks (around 0.1 and 0.3 ms) could be observed, and the ratio of their intensities followed the same trend as for papers. The only difference was in the position of the transition: for the paper, the appearance of the third peak occurred at 65% RH, while it appeared at 33% RH for the coated paper. The appearance of more mobile solid phases was accelerated by the chitosan coating, despite the very low amount of chitosan deposited on the papers.

This could be linked to the mechanical property measurements. Indeed, they were performed at 50% RH. At this RH,

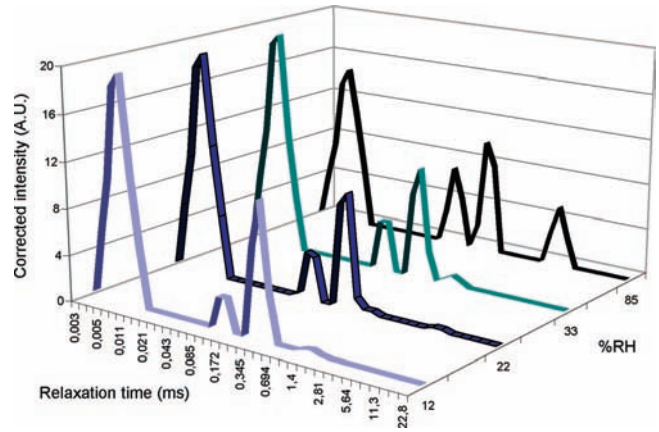

Figure 12. $T_{1\rho}$ relaxation spectra of Ahlstrom paper coated with chitosan at 12, 53, 65, and 85% RH from foreground to background.

only two peaks can be observed in the Ahlstrom paper spectrum, while a third peak related to a more mobile phase has already appeared in coated paper. Thus, this solid phase, probably due to hydrated and more mobile chitosan chains, could act as a plasticizer between the cellulose fibers, as suggested previously, and could explain the differences in the mechanical properties of the papers and the coated papers.

In conclusion, $T_{1\rho}$ measurements showed that a chitosan coating did not dramatically affect the global behavior of the solid matrix of the papers: despite the presence of chitosan in the paper matrix, the cellulose fibers network still drove the behavior of this network. Nevertheless, the difference of RH for the appearance of mobile solid phases could be linked to the slight differences between papers and coated papers through their mechanical properties.

Conclusion. The barrier properties against moisture and liquid water were evaluated on chitosan films, papers, and chitosan-coated papers, and their mechanical properties were investigated.

First, the chitosan-coated materials exhibited good moisture barrier properties, but not sufficient for food applications, and their surface hydrophilicity was too high. NMR-relaxometry studies showed that this was due to the hydrophilic character of chitosan, despite the very low amount of the aminopolysaccharide on the coated papers.

Second, this low chitosan content did not radically modify the mechanical properties of papers, as confirmed by NMR studies. Indeed, chitosan–paper bilayer structures were expected, but the resulting materials were systems of cellulose fibers embedded with chitosan.

Thus, a way to decrease the surface hydrophilicity and WVTR shall be found. Biocomposite formulations with fatty components or chitosan derivatizations with hydrophobic groups could be performed.

ACKNOWLEDGMENT

We gratefully acknowledge Professor Bernard De Jeso for low-resolution NMR assistance.

LITERATURE CITED

(1) Gallstedt, M.; Brottman, A.; Hedenqvist, M. S. Packaging-related properties of protein- and chitosan-coated paper. *Packag. Technol. Sci.* **2005**, *18*, 161–170.

(2) Mucha, M.; Miskiewicz, D. Chitosan blends as fillers for paper. *J. Appl. Polym. Sci.* **2000**, *77*, 3210–3215.
(3) Nada, A. M. A.; El-Sakhawy, M.; Kamel, S.; Eid, M. A. M.; Adel, A. M. Mechanical and electrical properties of paper sheets treated with chitosan and its derivatives. *Carbohydr. Polym.* **2006**, *63*, 113–121.
(4) Ravi Kumar, M. N. V. A review of chitin and chitosan applications. *React. Funct. Polym.* **2000**, *46*, 1–27.
(5) Desbrières, J. *Chitine et chitosane in L'actualité chimique*; Société Française de Chimie: Paris, 2002, 39–44.
(6) Bégin, A.; Van Calsteren, M. R. Antimicrobial films produced from chitosan. *Int. J. Biol. Macromol.* **1999**, *26*, 63–67.
(7) Devlieghere, F.; Vermeulen, A.; Debevere, J. Chitosan: antimicrobial activity, interactions with food components and applicability as a coating on fruits and vegetables. *Food Microbiol.* **2004**, *21*, 703–714.
(8) Park, H. J. Development of advanced edible coatings for fruits. Trends. *Food Sci. Technol.* **1999**, *10*, 254–260.
(9) Choi, W. Y.; Park, H. J.; Ahn, D. J.; Lee, J.; Lee, C. Y. Wettability of chitosan coating solution on Fuji apple ski. *J. Food Sci.* **2002**, *67*, 2668–2672.
(10) Guilbert, S.; Gontard, N.; Cuq, B. Technology and applications of edible protective films. *Packag. Technol. Sci.* **1995**, *8*, 339–346.
(11) Martin-Polo, M.; Mauguin, C.; Voilley, A. Hydrophobic films and their efficiency against moisture transfer. 1. Influence on the film preparation technique. *J. Agric. Food Chem.* **1992**, *40*, 881–888.
(12) Arvanitoyannis, I. S.; Nakayama, A.; Aiba, S. I. Chitosan and gelatin based edible films: state diagrams, mechanical and permeation properties. *Carbohydr. Polym.* **1998**, *37*, 371–382.
(13) Morillon, V.; Debeaufort, F.; Capelle, M.; Blond, G.; Voilley, A. Influence of the physical state of water on the barrier properties of hydrophilic and hydrophobic films. *J. Agric. Food Chem.* **2000**, *48*, 11–16.
(14) Varum, K. M.; Egelandsdal, B.; Ellekjaer, M. R. Characterizaion of partially *N*-acetylated chitosans by near infra-red spectroscopy. *Carbohydr. Polym.* **1995**, *28*, 187–193.
(15) Brugnerotto, J.; Lizardi, J.; Goycoolea, F. M.; Arguelles-Monal, W.; Desbrieres, J.; Rinaudo, M. An infrared investigation in relation with chitin and chitosan characterization. *Polymer* **2001**, *42*, 3659–3580.
(16) Partanen, R.; Marie, V.; MacNaughtan, W.; Forssell, P.; Farhat, I. ^{1}H NMR study of amylose films plasticised by glycerol and water. *Carbohydr. Polym.* **2004**, *56*, 147–155.
(17) Muller-Plathe, F. Different states of water in hydrogels. *Macromolecules* **1998**, *31*, 6721–6723.
(18) Mao, R.; Tang, J.; Swanson, B. G. Relaxation time spectrum of hydrogels by CONTIN analysis. *J. Food Sci.* **2000**, *65*, 374–381.
(19) Capitani, D.; Crescenzi, V.; De Angelis, A. A.; Segre, A. L. Water in hydrogels. An NMR study of water/polymer interactions in weakly cross-linked chitosan networks. *Macromolecules* **2001**, *34*, 4136–4144.
(20) Capitani, D.; Segre, A. L.; Attanasio, D.; Blicharska, B.; Focher, B.; Capretti, G. ^{1}H NMR relaxation study of paper as a system of cellulose and water. *Tappi J.* **1996**, *79*, 113–122.
(21) Capitani, D.; Emanuele, M. C.; Bella, J.; Segre, A. L.; Attanasio, D.; Focher, B.; Capretti, G. ^{1}H NMR relaxation study of cellulose and water interaction in paper. *Tappi J.* **1999**, *82*, 117–124.
(22) Srinivasa, P. C.; Ramesh, M. N.; Kumar, K. R.; Tharanathan, R. N. Properties of chitosan films prepared under different drying conditions. *J. Food Eng.* **2004**, *63*, 79–85.
(23) Kam, H. M.; Khor, E.; Lim, L. Y. Storage of partially deacetylated chitosan films. *J. Biomed. Mater. Res. (Appl. Biomater.)* **1999**, *48*, 881–888.
(24) Hwang, K. T.; Kim, J. T.; Jung, S. T.; Cho, G. S.; Park, H. J. Properties of chitosan-based biopolymer films with various degrees of deacetylation and molecular weights. *J. Appl. Polym. Sci.* **2003**, *89*, 3476–3484.
(25) Suyatma, N. E.; Copinet, A.; Tighzert, L.; Coma, V. Mechanical and barrier properties of biodegradable films made from chitosan and poly(lactic acid) blends. *J. Polym. Environ.* **2004**, *12*, 1–6.

Received for review March 1, 2007. Revised manuscript received June 24, 2007. Accepted July 18, 2007. Research funding was provided by the SustainPack European Program.

JF070595I